

Néel-VBS phase boundary of the extended J_1 - J_2 model with biquadratic interaction

Yoshihiro Nishiyama

*Department of Physics, Faculty of Science,
Okayama University, Okayama 700-8530, Japan*

(Dated: January 5, 2012)

Abstract

The J_1 - J_2 model with the biquadratic (plaquette-four-spin) interaction was simulated with the numerical-diagonalization method. Some limiting cases of this model have been investigated thoroughly. Taking the advantage of the extended parameter space, we survey the phase boundary separating the Néel and valence-bond-solid phases. According to the deconfined-criticality scenario, the singularity of this phase boundary is continuous, accompanied with unconventional critical indices. Diagonalizing the finite-size cluster with $N \leq 36$ spins, we observe a signature of continuous phase transition. Our tentative estimate for the correlation-length critical exponent is $\nu = 1.1(3)$. In order to elucidate a non-local character of criticality, we evaluated the Roombany-Wyld β function around the critical point.

I. INTRODUCTION

The deconfined criticality^{1–3} is arousing much attention recently.⁴ Naively,² the (ground-state) phase transition separating the Néel and valence-bond-solid (VBS) phases is discontinuous, because the adjacent phases possess distinctive order parameters such as the sublattice magnetization and the dimer-coverage pattern, respectively. However, according to the deconfined-criticality scenario, the transition is continuous, accompanied with novel critical indices;^{5–11} afterward, we make an overview on recent computer-simulation studies.

In this paper, we investigate an extended version of the J_1 - J_2 model^{12–14} [see Eq. (1)] by means of the numerical diagonalization method for the cluster with $N \leq 36$ spins. The extension of the parameter space, (J_2, Q) , permits us to investigate the above-mentioned criticality from a global viewpoint. A schematic phase diagram is presented in Fig. 1; details are explicated afterward. As mentioned above, the critical branch (dashed line) is our concern.

The Hamiltonian of the J_1 - J_2 model with the biquadratic interaction Q is given by

$$\mathcal{H} = J_1 \sum_{\langle ij \rangle} \mathbf{S}_i \cdot \mathbf{S}_j + J_2 \sum_{\langle\langle ij \rangle\rangle} \mathbf{S}_i \cdot \mathbf{S}_j - Q \sum_{[ijkl]} [(\mathbf{S}_i \cdot \mathbf{S}_j - 1/4)(\mathbf{S}_k \cdot \mathbf{S}_l - 1/4) + (\mathbf{S}_i \cdot \mathbf{S}_l - 1/4)(\mathbf{S}_j \cdot \mathbf{S}_k - 1/4)]. \quad (1)$$

Here, the quantum spin-1/2 operators $\{\mathbf{S}_i\}$ are placed at each square-lattice point i . The summations, $\sum_{\langle ij \rangle}$, $\sum_{\langle\langle ij \rangle\rangle}$, and $\sum_{[ijkl]}$, run over all possible nearest-neighbor pairs $\langle ij \rangle$, next-nearest-neighbor pairs $\langle\langle ij \rangle\rangle$, and plaquette spins $[ijkl]$, respectively; here, the arrangement of indices, $[ijkl]$, around a plaquette, \square , is $i_j \square_k^l$. The parameters, J_1 , J_2 , and Q , are the corresponding coupling constants. Hereafter, we consider J_1 as the unit of energy; namely, we set $J_1 = 1$. Both frustration and biquadratic interactions, J_2 and Q , stabilize the VBS phase.

In some limiting cases (subspaces), namely, either $Q = 0$ or $J_2 = 0$, the Hamiltonian (1) has been investigated extensively so far. The case of $Q = 0$, namely, the J_1 - J_2 model,¹⁵ has been analyzed with the series-expansion method^{15–18} and the numerical diagonalization method.^{18–22} (The quantum Monte Carlo method is inapplicable to such a frustrated magnetism because of the negative-sign problem.) The Néel, VBS, and collinear phases appear¹⁵ successively in the regimes, $J_2/J_1 \lesssim 0.4$, $0.4 \lesssim J_2/J_1 \lesssim 0.6$, and $0.6 \lesssim J_2/J_1$, respectively. The singularity²³ at $J_2/J_1 \approx 0.4$ (0.6) is continuous (discontinuous¹⁶). On the

one hand, the case of $J_2 = 0$, namely, the J - Q model^{24,25} (J_1 - Q model in our notation), admits the use of the quantum Monte Carlo method. The Néel phase turns into the VBS phase at a considerably large biquadratic interaction $Q/J \approx 25$.²⁴ This fact indicates that the antiferromagnetic order at $J_2 = 0$ is considerably robust against Q . Nevertheless, the large-scale quantum Monte Carlo simulation admits detailed analyses of criticality. The correlation-length critical exponent is estimated as $\nu = 0.78(3)$ (Ref. 24) and $\nu = 0.68(4)$ (Ref. 25). According to Ref. 26, logarithmic scaling corrections prevent us from taking the thermodynamic limit reliably. Possibly because of this difficulty, it is still controversial whether the singularity is continuous or belongs to a discontinuous one accompanied with an appreciable latent heat^{27–34}; see aforementioned Ref. 16 as well. Last, it has been mentioned that there have been reported a number of intriguing extinctions such as the third-neighbor interaction,³⁵ internal symmetry enlargement,³⁶ and spatial anisotropy.^{37–39} The dimer model^{40,41} is also a clue to the study of deconfined criticality.

In this paper, taking the advantage of the extended parameter space (J_2, Q) (see Fig. 1), we survey the critical branch in details. Scanning the parameter space, we found that around an intermediate regime $Q = 0.2$, the finite-size-scaling behavior improves significantly. Around this optimal regime, we carry out finite-size-scaling analyses

The rest of this paper is organized as follows. In Sec. II, we present the simulation results. Technical details are explicated. In Sec. III, we address the summary and discussions.

II. NUMERICAL RESULTS

In this section, we present the numerical results for the J_1 - J_2 - Q model, Eq. (1). We employ the exact-diagonalization method for the cluster with $N (= L^2) \leq 6^2$ spins. Our aim is to clarify the nature of the phase boundary separating the Néel and VBS phases. For that purpose, we scrutinize the excitation gap

$$\Delta E = E_{[(0,\pi),0,+,+,+]} - E_{[(0,0),0,+,+,+]}. \quad (2)$$

Here, the variable E_α denotes the ground-state energy within the sector (subspace) specified by the set of quantum numbers, $\alpha = (\vec{k}, S^z, \pm, \pm, \pm)$. These quantum numbers $(\vec{k}, S^z, \pm, \pm, \pm)$ are associated with the symmetry groups such as translation along the rectangular edges, internal-spin z -axis rotation (total-spin conservation along the z axis),

internal-spin inversion ($S_i^z \leftrightarrow -S_i^z$), $\theta = \pi$ lattice rotation, and lattice inversion, respectively. These symmetry groups commute mutually, because we restrict ourselves within the sector with $k_x = 0$ and $S^z = 0$. The excitation gap, Eq. (2), opens (closes) for the Néel (VBS) phase in the thermodynamic limit. (The degeneracy in the VBS phase corresponds to the translationally-invariant dimer-coverage patterns.) The excitation branch (2) does not correspond to the first energy gap: There appear numerous low-lying excitations due to the spontaneous-symmetry breakings in both Néel and VBS phases. Here, aiming to discriminate these phases clearly, we look into an excitation branch (2), which is a key ingredient of the finite-size-scaling analysis.

A. Survey of the phase boundary between the VBS and Néel phases

In Fig. 2, we plot the scaled energy gap $L\Delta E$ for $Q = 0.2$, various J_2 , and $N = 4$, 16, and 36. Here, the variable $L (= \sqrt{N})$ denotes the linear dimension of the cluster. The intersection point of the curves indicates a location of the critical point. We see that a transition occurs at $J_2 \approx 0.3$.

In order to estimate the transition point precisely, in Fig. 3, we plot the approximate critical point $J_{2c}(L_1, L_2)$ for $2/(L_1 + L_2)$ with $2 \leq L_1 < L_2 \leq 6$; the parameters are the same as those of Fig. 2. Here, the approximate critical point $J_{2c}(L_1, L_2)$ denotes a scale-invariant point with respect to a pair of system sizes (L_1, L_2) . Namely, it satisfies the relation

$$L_1\Delta E(L_1)|_{J_2=J_{2c}(L_1, L_2)} = L_2\Delta E(L_2)|_{J_2=J_{2c}(L_1, L_2)}. \quad (3)$$

The least-squares fit to the data of Fig. 3 yields an estimate $J_{2c} = 0.273(12)$ in the thermodynamic limit $L \rightarrow \infty$. Replacing the abscissa scale with $1/L^2$, we obtain an alternative estimate $J_{2c} = 0.3095(91)$. The discrepancy between these estimates, $\approx 3.7 \cdot 10^{-2}$, appears to dominate the insystematic (statistical) error, $\approx 10^{-2}$. Considering the former as an indicator of the error margin, we estimate the transition point $J_{2c} = 0.273(37)$.

We carried out similar analyses for various values of Q . The results are shown in Fig. 4. The error margin is suppressed around an intermediate regime $Q \sim 0.1$. As a matter of fact, in Fig. 5, we show that the scaling behavior becomes optimal around $Q \approx 0.2$. (Such a redundancy is a benefit of the parameter-space extension.) On the contrary, the error

margins get enhanced around the multi-critical point as well as in the large- Q regime.

As mentioned in the Introduction, the limiting cases, $Q = 0$ and $J_2 = 0$, have been studied extensively.^{15,24} In Ref. 15, The transition point $(J_2, Q) \approx (0.4, 0)$ was reported. This result agrees with ours. On the contrary, the transition point²⁴ $(J_2, Q) \approx (0, 25)$ is not reproduced by the present approach. This discrepancy may be attributed to the logarithmic corrections²⁶ inherent in the subspace $J_2 = 0$; these corrections prevent us from taking the thermodynamic limit reliably. Around $Q \approx 0$, there arise pronounced scaling corrections, which cannot be appreciated properly; this regime would not be accessible by the numerical diagonalization method. As a matter of fact, the Q -driven VBS state is so unstable that a considerably weak antiferromagnetic interaction $J_1 = 0.04$ destroys VBS immediately. This difficulty is remedied by the inclusion of the magnetic frustration J_2 , which appears to stabilize VBS significantly (Fig. 4), and recover an applicability of the diagonalization method.

Last, we make a comment. The present simulation cannot rule out a possibility of the discontinuous phase transition. Even in such a case, the phase boundary determined through the criterion, Eq. (3), makes sense, albeit the value of $L\Delta E$ at the transition point no longer converges to a universal value (critical amplitude).

B. Correlation-length critical exponent

In this section, we estimate the correlation-length critical exponent ν . In Fig. 5, we plot the approximate critical exponent

$$\nu(L_1, L_2) = \frac{\ln(L_1/L_2)}{\ln\{\partial_J[L_1\Delta E(L_1)]/\partial_J[L_2\Delta E(L_2)]\}|_{J_2=J_{2c}(L_1, L_2)}}, \quad (4)$$

for $2/(L_1 + L_2)$ and $2 \leq L_1 < L_2 \leq 6$. The parameters are the same as those of Fig. 2. The least-squares fit to these data yields $\nu = 1.094(26)$ in the thermodynamic limit. In order to appreciate possible systematic errors, we made an alternative extrapolation with the $1/L^2$ -abscissa scale. Thereby, we arrive at $\nu = 1.087(14)$. In this (optimal) parameter space, $Q = 0.2$, the systematic error (deviation between different abscissa scales) appears to be negligible. On the one hand, at $Q = 0.3$, we estimated $\nu = 0.901(21)$ and $0.988(17)$ through the $1/L$ - and $1/L^2$ -extrapolation schemes, respectively. The discrepancy (systematic error) appears to be enhanced by the scaling (possibly, logarithmic²⁶) corrections. At $Q = 0.1$,

via the $1/L$ - and $1/L^2$ -extrapolation schemes, we arrive at $\nu = 1.316(87)$ and $1.198(55)$, respectively. Both systematic and insystematic errors get enhanced in the proximity to the multicritical point. Considering these deviations of various characters as an indicator of the error margin, we estimate the critical exponent as

$$\nu = 1.1(3). \quad (5)$$

A validity of the scaling analysis is considered in the next section.

C. Non-local behavior of the β function

In Fig. 6, we plot the β function, $\beta_{L_1 L_2}^{RW}(J_2)$, for $Q = 0.2$, various J_2 , and $(L_1, L_2) = (+)$ $(2, 4)$, (\times) $(4, 6)$, and $(*)$ $(2, 6)$. Here, we calculated the β function with the Roomany-Wyld formula⁴²

$$\beta_{L_1 L_2}^{RW}(J_2) = \frac{1 + \ln(\Delta E(L_1)/\Delta E(L_2))/\ln(L_1/L_2)}{\sqrt{\partial_{J_2} \Delta E(L_1) \partial_{J_2} \Delta E(L_2) / \Delta E(L_1) \Delta E(L_2)}}, \quad (6)$$

for a pair of system sizes (L_1, L_2) .

The β function elucidates a non-local character of the criticality. In the vicinity of the critical point J_{2c} , the β function falls into a linearized formula

$$\beta(J_2) = \frac{1}{\nu}(J_{2c} - J_2), \quad (7)$$

with the correlation-length critical exponent ν . In Fig. 6, we present the theoretical prediction $\beta = (0.273 - J)/1.1$ (dotted line); here, the critical parameters, $J_{2c} = 0.273$ and $\nu = 1.1$, are estimated in the preceding sections. The behavior of $\beta_{L_1 L_2}^{RW}$ is consistent with the theoretical prediction for a considerably wide range of J_2 , validating our treatment. In particular, the linearity of $\beta_{L_1 L_2}^{RW}$ is remarkable, suggesting that scaling corrections are eliminated satisfactorily, at least, around $Q = 0.2$. Possibly, the J_2 -driven phase transition, rather than the Q -driven transition, is reasonable in the sense of the renormalization-group flow.

D. Ground-state energy: An indication of the VBS-collinear phase transition

In Fig. 7, we present the ground-state energy per unit cell, E_g/N , with $N = 36$ for $Q = 0.2$ and various J_2 . From the figure, we observe a cusp-like anomaly around $J_2 \approx 0.7$. This

anomaly indicates an onset of the first-order phase transition between the VBS and collinear phases. Making similar analyses for various values of Q , we obtained a schematic feature of the VBS-collinear phase boundary as shown in Fig. 1. Character of the multicritical point is unclear.

III. SUMMARY AND DISCUSSIONS

The phase diagram of the extended J_1 - J_2 model with the biquadratic interaction Q , Eq. (1), was investigated by means of the numerical diagonalization method for $N \leq 36$. Taking the advantage of the extended parameter space, (J_2, Q) , we surveyed the critical branch separating the Néel and VBS phases (Fig. 4) in particular. The finite-size corrections appear to be suppressed around an intermediate regime $Q \approx 0.2$. Encouraged by this finding, we analyzed the criticality around $Q \approx 0.2$ with the finite-size-scaling method. As a result, we estimate the correlation-length critical exponent $\nu = 1.1(3)$. A non-local feature of the β function is accordant with the theoretical prediction (Fig. 6), giving support to our treatment.

As a reference, we overview related studies. For the J - Q model (square-lattice anti-ferromagnet with the biquadratic interaction), the estimates, $\nu = 0.78(3)$ (Ref. 24) and $\nu = 0.68(4)$ (Ref. 25), were reported. As for the spatially-anisotropic spin systems, the exponent $\nu = 0.80(15)$ (Ref. 38) and $\nu = 0.92(10)$ (Ref. 39) were obtained. These results are to be compared with $\nu = 0.7112(5)$ (Ref. 43) for the $d = 3$ Heisenberg universality class. Our result indicates a tendency toward an enhancement for the correlation-length critical exponent, as compared to that for the $d = 3$ Heisenberg universality class.

According to Ref. 44, information on the deconfined criticality can be drawn from the details of the multi-critical point. This viewpoint would provide an evidence whether the criticality belongs to the deconfined criticality; at present, it is not conclusive whether the Néel-VBS transition belongs to the deconfined criticality. This problem will be addressed in future study.

¹ T. Senthil, A. Vishwanath, L. Balents, S. Sachdev, and M. P. A. Fisher, Science **303**, 1490 (2004).

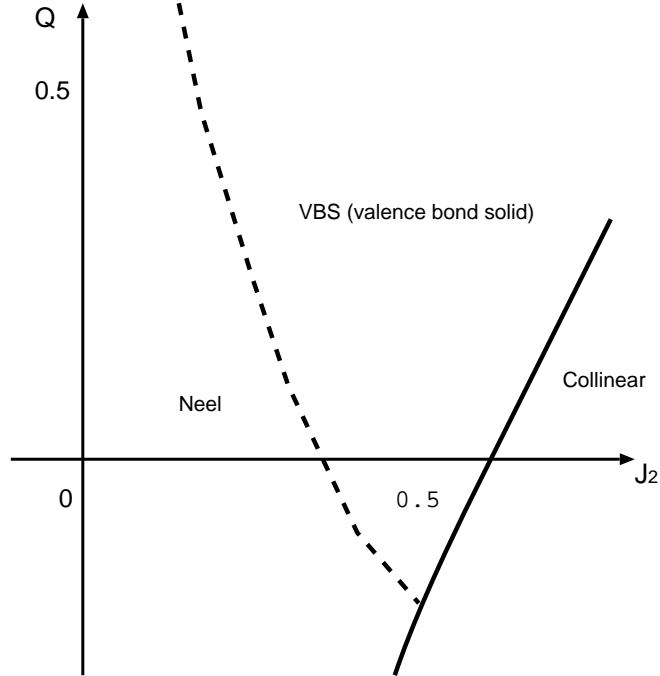


FIG. 1. A schematic (ground-state) phase diagram for the J_1 - J_2 - Q model (1) is presented. The solid (dashed) line stands for the phase boundary of discontinuous (continuous) character. We investigate the phase boundary separating the Néel and VBS phases. Details of the multi-critical point and the VBS-collinear phase boundary are uncertain.

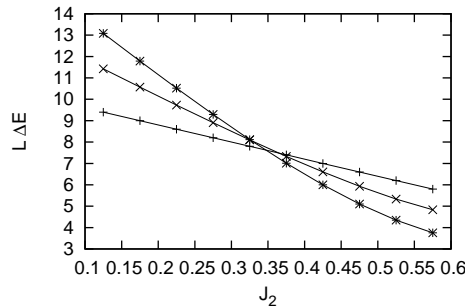


FIG. 2. The scaled energy gap $L\Delta E$ is plotted for the next-nearest-neighbor interaction J_2 and the system size $L = (+) 2, (\times) 4$, and $(*) 6$. The biquadratic interaction is fixed to $Q = 0.2$. The data indicate an onset of continuous phase transition around $J_2 \approx 0.3$.

² T. Senthil, L. Balents, S. Sachdev, A. Vishwanath, and M. P. A. Fisher, Phys. Rev. B **70**, 144407 (2004).

³ M. Levin and T. Senthil, Phys. Rev. B **70**, 220403 (2004).

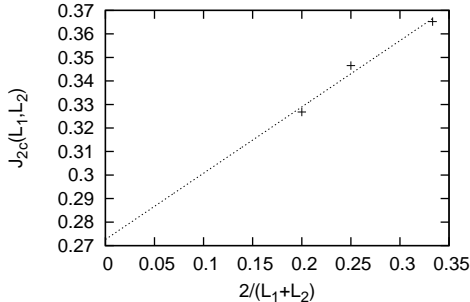


FIG. 3. The approximate critical point $J_{2c}(L_1, L_2)$ (3) is plotted for $2/(L_1 + L_2)$ with $2 \leq L_1 < L_2 \leq 6$. The parameters are the same as those of Fig. 2. The least-squares fit to these data yields $J_{2c} = 0.273(12)$ in the thermodynamic limit. A possible systematic error is considered in the text.

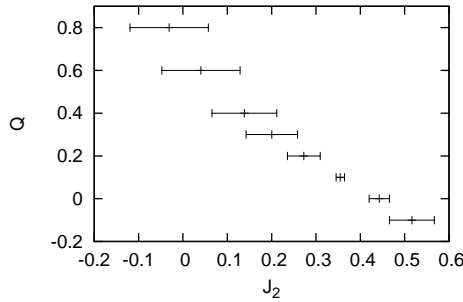


FIG. 4. The phase boundary between the Néel and VBS phases (critical branch) is presented.

- ⁴ R. R. P. Singh, Physics **3**, 35 (2010).
- ⁵ O. I. Motrunich and A. Vishwanath, Phys. Rev. B **70**, 075104 (2004).
- ⁶ A. Tanaka and X. Hu, Phys. Rev. B **74**, 140407(R) (2006).
- ⁷ G.-Z. Liu, Phys. Rev. B **71**, 172501 (2005).
- ⁸ R. Dillenschneider and J. Richert, Phys. Rev. B **73**, 224443 (2006).
- ⁹ P. Ghaemi and T. Senthil, Phys. Rev. B **73**, 054415 (2006).
- ¹⁰ I. O. Thomas and S. Hands, Phys. Rev. B **75**, 134516 (2007).
- ¹¹ D. H. Kim, P. A. Lee, and X.-G. Wen, Phys. Rev. Lett. **79**, 2109 (1997).
- ¹² M.P. Gelfand, R.R.P. Singh, and D.A. Huse, Phys. Rev. B **40**, 10801 (1989).
- ¹³ E. Dagotto and A. Moreo, Phys. Rev. Lett. **63**, 2148 (1989).
- ¹⁴ H. J. Schulz and T. A. L. Ziman, Europhy. Lett. **18**, 355 (1992).
- ¹⁵ J. Oitmaa and Z. Weihong, Phys. Rev. B **54**, 3022 (1996).

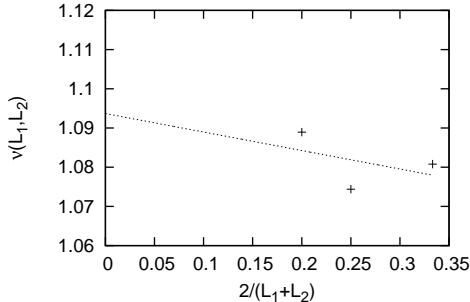


FIG. 5. The approximate critical exponent $\nu(L_1, L_2)$ (4) is plotted for $2/(L_1 + L_2)$ with $2 \leq L_1 < L_2 \leq 6$. The parameters are the same as those of Fig. 2. The least-squares fit to these data yields $\nu = 1.094(26)$ in the thermodynamic limit. A possible systematic error is considered in the text.

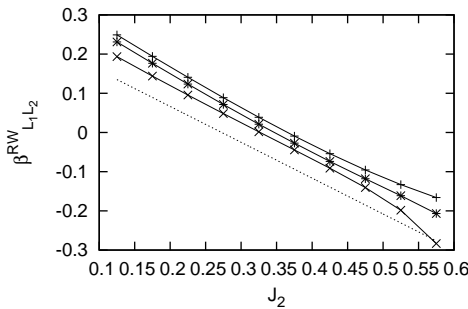


FIG. 6. The beta function $\beta_{L_1 L_2}^{RW}$ (6) is plotted for $Q = 0.2$, various J_2 , and $(L_1, L_2) = (+)$ (2, 4), (\times) (4, 6), and $(*)$ (2, 6). For a comparison, we present a theoretical prediction $\beta = (0.273 - J_2)/1.1$ (dotted line); see text for details. We see that the β function follows the theoretical prediction for a wide range of J_2 .

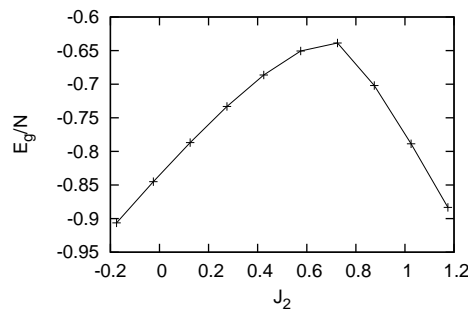


FIG. 7. The ground-state energy per unit cell E_g/N with $N = 36$ is presented for $Q = 0.2$ and various J_2 .

- ¹⁶ J. Sirker, Z. Weihong, O.P. Sushkov, and J. Oitmaa, Phys. Rev. B **73**, 184420 (2006).
- ¹⁷ R. Darradi, O. Derzhko, R. Zinke, J. Schulenburg, S.E. Krüger, and J. Richter, Phys. Rev. B **78**, 214415 (2008).
- ¹⁸ J. Richter, R. Darradi, J. Schulenburg, D.J.J. Farnell, and H. Rosner, Phys. Rev. B **81**, 174429 (2010).
- ¹⁹ D. Poilblanc, A. Läuchli, M. Mambrini, and F. Mila, Phys. Rev. B **73**, 100403(R) (2006).
- ²⁰ L. Capriotti, F. Becca, A. Parola, and S. Sorella, Phys. Rev. B **67**, 212402 (2003).
- ²¹ P. Sindzingre, C. Lhuillier, and J.-B. Fouet, Int. J. Mod. Phys. B **17**, 5031 (2003).
- ²² J. Richter and J. Schulenburg, Eur. Phys. J. B **73**, 117 (2010).
- ²³ J.-F. Yu and Y.-J. Kao, arXiv: 1108.3393.
- ²⁴ A. W. Sandvik, Phys. Rev. Lett **98**, 227202 (2007).
- ²⁵ R. G. Melko and R. K. Kaul, Phys. Rev. Lett. **100**, 017203 (2008).
- ²⁶ A. W. Sandvik, Phys. Rev. Lett. **104**, 177201 (2010).
- ²⁷ Valeri N. Kotov, Dao-Xin Yao, A. H. Castro Neto, and D. K. Campbell, Phys. Rev. B **80**, 174403 (2009).
- ²⁸ L. Isaev, G. Ortiz, and J. Dukelsky, Phys. Rev. B **82**, 136401 (2010).
- ²⁹ Valeri N. Kotov, D. X. Yao, A. H. Castro Neto, and D. K. Campbell, Phys. Rev. B **82**, 136402 (2010).
- ³⁰ L. Isaev, G. Ortiz, and J. Dukelsky, J. Phys.: Condens. Matter **22**, 016006 (2010).
- ³¹ A. Kuklov, N. Prokof'ev, and B. Svistunov, Phys. Rev. Lett. **93**, 230402 (2004).
- ³² A.B. Kuklov, M. Matsumoto, N.V. Prokof'ev, B.V. Svistunov, and M. Troyer, Phys. Rev. Lett. **101**, 050405 (2008).
- ³³ F.-J. Jiang, M. Nyfeler, S. Chandrasekharan, and U.-J. Wiese, J. Stat. Mech., P02009 (2008).
- ³⁴ K. Krüger and S. Scheidl, Europhys. Lett. **74**, 896 (2006).
- ³⁵ J. Reuther, P. Wölfle, R. Darradi, W. Brenig, M. Arlego, and J. Richter, Phys. Rev. B **83**, 064416 (2011).
- ³⁶ N. Kawashima and Y. Tanabe, Phys. Rev. Lett. **98**, 057202 (2007).
- ³⁷ K. Harada, N. Kawashima, and M. Troyer, J. Phys. Soc. Japan **76**, 013703 (2007).
- ³⁸ Y. Nishiyama, Phys. Rev. B **79**, 054425 (2009).
- ³⁹ Y. Nishiyama, Phys. Rev. B **83**, 054417 (2011).
- ⁴⁰ D. Charrier and F. Alet, Phys. Rev. B **82**, 014429 (2010).

- ⁴¹ S. Papanikolaou and J.J. Betouras, Phys. Rev. Lett. **104**, 045701 (2010).
- ⁴² H.H. Roomany and H.W. Wyld, Phys. Rev. D **21**, 3341 (1980).
- ⁴³ M. Campostrini, M. Hasenbusch, A. Pelissetto, P. Rossi, and E. Vicari, Phys. Rev. B **65**, 144520 (2002).
- ⁴⁴ C. Xu and S. Sachdev, Phys. Rev. B **79**, 064405 (2009).